



First-principles study of density, viscosity, and diffusion coefficients of liquid MgSiO₃ at conditions of the Earth's deep mantle

J. T. K. Wan,^{1,2} T. S. Duffy,³ S. Scandolo,⁴ and R. Car¹

Received 31 October 2005; revised 11 September 2006; accepted 25 October 2006; published 28 March 2007.

[1] Constant-pressure constant-temperature ab initio molecular dynamics simulations at high temperatures have been used to study MgSiO₃, the major constituent of the Earth's lower mantle to conditions of the Earth's core-mantle boundary. The calculated equilibrium volumes and densities are compared with simulations using an orthorhombic perovskite configuration under the same conditions. For molten MgSiO₃, we have determined the diffusion coefficients and shear viscosities at different thermodynamic conditions. Our results provide new constraints on the properties of molten MgSiO₃ at conditions near the core-mantle boundary. The volume of the liquid is greater than that of the solid throughout the pressure-temperature conditions examined, and the volume change on fusion ranges from 5% at 88 GPa and 3500 K to 2.9% at 120 GPa and 5000 K. Existing experimental constraints on solid-liquid partition coefficients for Fe suggest that Fe is preferentially partitioned into the liquid. Such enrichment of Fe increases the density of the liquid, thus allowing the possibility of negatively buoyant melts from (Mg,Fe)SiO₃ perovskite compositions at deep lower mantle conditions for plausible values of solid-liquid partition coefficients for Fe. At 120 GPa and 4500–5000 K, the diffusion coefficient of liquid MgSiO₃ is $2\text{--}3 \times 10^{-5} \text{ cm}^2/\text{s}$ and the diffusion rates of the different chemical species are similar. The shear viscosity is estimated using Zwanzig's formula to be 19–31 cP under these conditions. On the basis of our calculated diffusivities, MgSiO₃ is above the glass transition temperature at 120 GPa and 4500 K.

Citation: Wan, J. T. K., T. S. Duffy, S. Scandolo, and R. Car (2007), First-principles study of density, viscosity, and diffusion coefficients of liquid MgSiO₃ at conditions of the Earth's deep mantle, *J. Geophys. Res.*, 112, B03208, doi:10.1029/2005JB004135.

1. Introduction

[2] Melting is a ubiquitous process in planetary interiors and one of the dominant mechanisms for thermal transport and chemical differentiation in planets. Knowledge of the properties of silicate liquids are thus necessary for understanding a wide range of geophysical phenomena related to the deep Earth and its origin and evolution. (Mg,Fe)SiO₃ perovskite is the most abundant mineral in the Earth's deep mantle. Here we report ab initio simulation of the properties of liquid MgSiO₃ at conditions corresponding to the deep interior of the Earth.

[3] There are a number of lines of evidence that strongly indicate the Earth (and other terrestrial planets) were partially or wholly molten, at least at certain intervals, during the accretion process [Stevenson, 1989; Solomatov, 2000]. The subsequent cooling and crystallization of a magma ocean might have led to the chemical differentiation of the mantle [Ohtani, 1985]. Thus understanding the dynamics of a terrestrial magma ocean is essential to understanding the initial conditions for the subsequent thermal and chemical evolution of the Earth. The liquid viscosity and its depth dependence are among the important parameters that characterize an early (liquid-rich) magma ocean [Solomatov, 2000] and melt/crystal density inversions could greatly modify the structure and cooling history of such an ocean [Solomatov, 2000]. At present, only low-pressure experimental data or calculations mainly based on empirical potentials have been used to constrain these models [Wasserman et al., 1993; Dingwell et al., 2004; Liebske et al., 2005].

[4] In the present Earth, the existence of small degrees (<1%) of partial melt has been suggested as an explanation for the strong relative variations of shear velocity relative to compressional ($\partial \ln V_S / \partial \ln V_P$) velocity in the deep lower mantle [Duffy and Ahrens, 1992]. In the D'' region at the

¹Department of Chemistry and Princeton Institute for the Science and Technology of Materials, Princeton University, Princeton, New Jersey, USA.

²Now at Department of Physics, Chinese University of Hong Kong, Hong Kong.

³Department of Geosciences and Princeton Institute for the Science and Technology of Materials, Princeton University, Princeton, New Jersey, USA.

⁴Adbus Salam International Centre for Theoretical Physics and National Simulation Center of the Italian Istituto Nazionale per la Fisica della Materia, Trieste, Italy.

base of the mantle, a seismic ultralow-velocity zone (ULVZ) of thickness 5–40 km has been detected locally on top of the core-mantle boundary [Garnero *et al.*, 1993; Revenaugh and Meyer, 1997; Helmberger *et al.*, 2000; Wen and Helmberger, 1998]. These regions are characterized by seismic compressional and shear velocity reductions of ~10% and ~30%, respectively. The presence of relatively large degrees of partial melt (~5–30%) has been proposed as the most plausible explanation for these features [Williams and Garnero, 1996]. There is also evidence for smaller shear velocity reductions in D'', plausibly consistent with lesser amounts of partial melt at depths as great as 300 km above the core mantle boundary [Wen *et al.*, 2001].

[5] The presence of melt in the deep mantle can greatly affect a number of physical properties of the region. The viscosity of the melt may strongly modify heat transport and convective circulation within the boundary layer [Williams and Garnero, 1996]. The presence of a partially molten layer suggests that the density contrast between solid and melt should be small. The buoyancy of the melt will be controlled by the intrinsic density difference, as well as compositional differences (i.e., Fe enrichment) between the melt and solid. Density inversions between silicate melts and equilibrium liquidus crystals have been extensively studied at upper mantle conditions [Agee, 1998; Rigden *et al.*, 1984; Suzuki and Ohtani, 2003; Sakamaki *et al.*, 2006; Matsukage *et al.*, 2005]. However, there are only limited constraints on possible density inversions under conditions of the Earth's lower mantle. It has been proposed on the basis of laboratory measurements to 15 GPa that basaltic melts may become denser than mantle peridotite at conditions near the base of the mantle [Ohtani and Maeda, 2001]. However, these results are subject to considerable uncertainty due to the long extrapolations involved. More direct determination of physical properties of the components of deep mantle melts is needed.

[6] Recent developments in the atomistic simulation of solids and liquids, based on the full solution of the quantum mechanical equations for the electrons, allow the theoretical study from first principles, i.e., without empirical or adjustable parameters, of the structural, thermal, and elastic properties of minerals at arbitrary conditions of pressure and temperature. Recent works have addressed successfully the thermoelastic properties of solid MgSiO₃ perovskite at Earth's mantle conditions [Karki *et al.*, 1997, 2000; Oganov *et al.*, 2001a, 2001b; Wentzcovitch *et al.*, 2004]. Here we focus on the properties of liquid MgSiO₃ at high pressures, which we study using first-principles molecular dynamics at constant pressure. We determine liquid densities and compare them with solid perovskite densities at similar conditions to extract melting properties. We also calculate or estimate dynamical properties of liquid MgSiO₃ such as diffusion and viscosity. Other studies that used first-principles molecular dynamics simulations to examine MgSiO₃ and MgO liquids were also recently reported [Stixrude and Karki, 2005; Karki *et al.*, 2006].

2. Technical Details

[7] Ab initio molecular dynamics (AIMD) simulations [Car and Parrinello, 1985] were performed using density functional theory [Hohenberg and Kohn, 1964; Kohn and

Sham, 1965] within the generalized gradient approximation (GGA) [Perdew *et al.*, 1996]. We use ultrasoft pseudopotentials [Vanderbilt, 1990] for O and norm-conserving pseudopotentials [Troullier and Martins, 1991] for Mg and Si. Nonlinear core corrections [Louie *et al.*, 1982] were used for Mg. Kohn-Sham orbitals were expanded in plane waves with a kinetic energy cut off of 30 Ry. The simulation cell contained 80 atoms (16 MgSiO₃ units) and a time step of 13 atomic time units was used (~0.31 fs). The simulations were performed in constant-pressure constant-temperature (NPT) statistical ensemble: variable-cell dynamics was used to impose the required pressure [Parrinello and Rahman, 1980], and the temperature was controlled by Nosé thermostat technique [Nosé, 1984; Hoover, 1985]. The variable-cell dynamics allows the cell parameters to be optimized automatically during simulation. The fictitious kinetic energy of the electronic wave functions was controlled by the scheme proposed by Blöchl and Parrinello [1992]. For simulations of the solid phase the first 0.5 ps of the simulations were discarded and statistical averaging was then carried out for at least 2 ps. The liquid configuration was obtained by heating the system to 10,000 K and then decreasing the temperature to 5000 K in a total time of 1 ps. Depending on the thermodynamic condition, the first 2–4 ps of the liquid simulations were discarded, and then the simulations were run for additional 8–12 ps to obtain sufficient statistical data for the calculation of the diffusion coefficient [Allen and Tildesley, 1987].

[8] The properties of MgSiO₃ liquid have also been the subject of another recent study using first-principles molecular dynamics simulations [Stixrude and Karki, 2005]. Our methods differ from this other work in some aspects including the choice of exchange correlation function, the statistical ensemble taken and the way the atomic trajectories were generated. In their recent work, Stixrude and Karki [2005] used the local density approximation (LDA) to approximate the exchange correlation; fixed-volume unit cells were used to ensure constant-volume constant-temperature (NVT) statistical ensemble, and the atomic trajectories were generated by Born-Oppenheimer molecular dynamics. In addition, we calculate the diffusivity and shear viscosity of MgSiO₃ liquid which was not contained in the other work. We also note our work focuses exclusively on deep lower mantle conditions (88–135 GPa, 3500–5000 K) and provides dense data coverage for this region.

[9] To test convergence of volumes, we performed both 160-atom and 80-atom simulations at 5000 K and 120 GPa and found that the calculated volumes were unchanged within statistical uncertainties. The statistical deviations in volume were found to be within 1.9% in all simulations. To justify the validity of our simulations, we performed an ambient pressure simulation for the perovskite structure at 300 K and the calculated molar volume of MgSiO₃ is 25.8 cm³. This is consistent to the calculated volume (25.3 cm³) using GGA by Oganov *et al.* [2001a]. These calculated values are 5% higher than the experimental values (24.5 cm³). Typically, density functional theory (DFT)-GGA calculations overestimate cell parameters by 2%, thus our calculated ambient solid volume is within the typical DFT-GGA calculation error. Recent work by Oganov *et al.* [2001a] suggests that a DFT-calculated equation of state (EOS) can mimic an experimental EOS by applying a

Table 1. Calculated Properties of MgSiO₃ at 3500 K as a Function of Pressure Using Solid Perovskite and Liquid Configurations^a

P , GPa	Solid Perovskite		Liquid		
	V_S , Å ³	ρ_S , g/cm ³	V_L , Å ³	ρ_L , g/cm ³	$\Delta V/V_S$, %
88	140.79	4.72	147.76	4.50	4.96
93	139.08	4.78	145.30	4.57	4.47
100	137.26	4.84	142.10	4.67	3.52
110	134.79	4.93	138.68	4.79	2.89
120	132.01	5.03	135.36	4.91	2.54
135	128.82	5.16	131.76	5.04	2.29

^aFor liquid configuration at 88 GPa, atoms are diffusive and the estimated diffusion coefficient is 1.14×10^{-5} cm²/s.

constant shift of pressure to it. However, as one of the main purpose of this work is to compare the difference in volumes of solid and liquid MgSiO₃ by using first-principles approaches. The application of a pressure correction would introduce extra artifacts to the calculations. Hence we would not employ the pressure correction in this work.

[10] The diffusion coefficient (D) is estimated by calculating the mean square displacement, $\langle \delta R^2(t) \rangle$, of the atoms as a function of time. The diffusion coefficient is given by the Einstein relation [Allen and Tildesley, 1987]:

$$D \approx \lim_{t \rightarrow \infty} \frac{1}{6t} \langle |\mathbf{r}(t_0 + t) - \mathbf{r}(t_0)|^2 \rangle = \lim_{t \rightarrow \infty} \frac{1}{6t} \langle \delta R^2(t) \rangle. \quad (1)$$

The calculated mean square displacements were fitted to a straight line:

$$\langle \delta R^2(t) \rangle \approx 6Dt + b. \quad (2)$$

The uncertainty of D is given by the asymptotic error when fitting equation (2). It should be noted that $\langle \delta R^2(t) \rangle$ is obtained by taking the average over time origins t_0 for, say, a period of t_{ens} . In practice, t_{ens} has to be large enough to ensure statistical accuracy and the correlation time t has to be smaller than t_{ens} . Typically, $t_{\text{ens}} > 3t$ [Allen and Tildesley, 1987]. Hence the total simulation time t_{total} must exceed the sum of t and t_{ens} , i.e., $t_{\text{total}} > t + t_{\text{ens}}$. In the case of solids, where no diffusion is observed in the timescale of a simulation, $D = 0$ and the constant b coincides with the Debye-Waller factor, which could in principle be extracted from the intensity of the peaks in diffraction experiments.

[11] The viscosity (η) is estimated using the generalized Debye-Stokes-Einstein formula derived by Zwanzig [1983]:

$$\frac{D\eta}{k_B T n^{1/3}} = 0.0658(2 + \eta/\eta_l) = C_l. \quad (3)$$

Here $n = N/V$ is the number density of the atoms. The constant C_l depends on the ratio of the shear viscosity (η) to the longitudinal viscosity (η_l). Although these numbers are not actually available, C_l has bounds that can vary between 0.132 and 0.181. In our work, we adopt a typical value of $C_l = 0.171$. The upper and lower bounds of C_l result in uncertainties of -23% and $+6\%$ in η , respectively. Wasserman et al. [1993] studied the transport properties of perovskite melts by molecular dynamics under high temperatures (3500–6000 K) and pressures (5.1–78 GPa) and their results agreed reasonably well with Zwanzig's formula. The general validity of Zwanzig's formula has

been studied in detail in other systems [March and Tosi, 1999; Bagchi, 2001; Gezelter et al., 1999].

3. Simulation Results

3.1. Materials Properties at High Pressures and Temperatures

[12] The calculated equilibrium volumes of four MgSiO₃ units (20 atoms) at 3500 K as a function of pressure are given in Table 1. The results are shown in Figure 1 (top). Our simulation results agree well with the AIMD-fitted

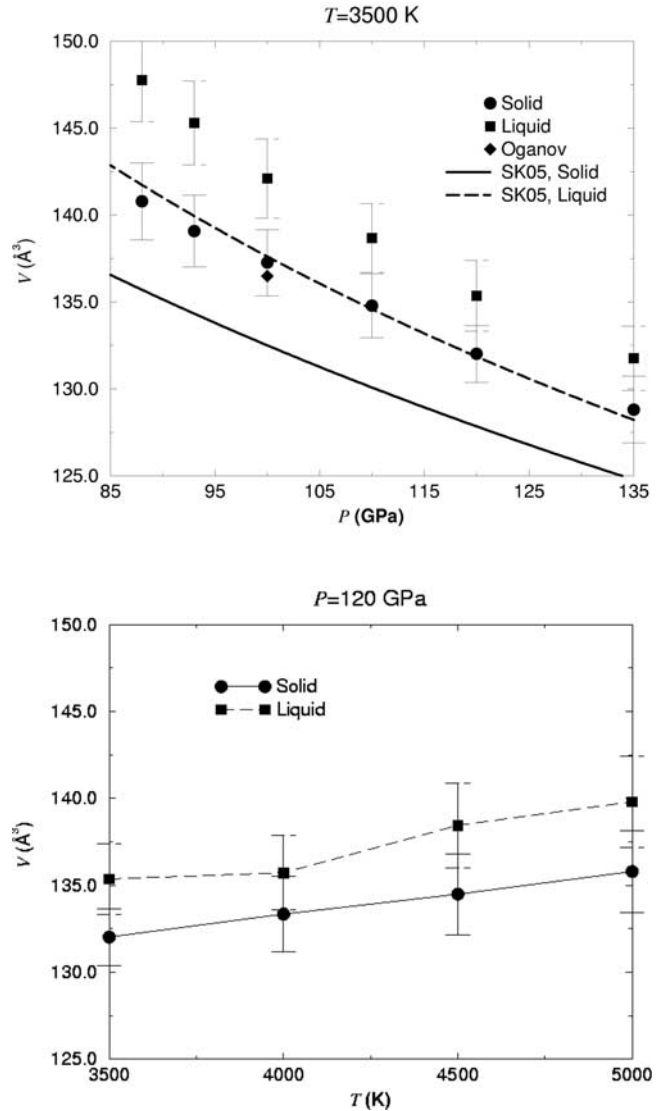


Figure 1. (top) Equations of state of solid and molten MgSiO₃ at 3500 K. Our results (symbols) are compared with values from the Mie-Grüneisen equation of state (bold solid and dashed lines) of Stixrude and Karki [2005] (SK05). Our equations of state are consistently different from the SK05 results by ~ 18 GPa (solid) and ~ 14 GPa (molten). The AIMD calculation of solid perovskite by Oganov et al. [2001a] is also shown. (bottom) Volumes of solid and molten MgSiO₃ at different temperatures. Pressure is fixed at 120 GPa. Note the difference between $T > 4500$ K and $T < 4000$ K. Lines serve only to connect data points. Errors in volumes are within 2%.

Table 2. Calculated Materials Properties of MgSiO₃ at 120 GPa as a Function of Temperature Using Solid Perovskite and Liquid Configurations

T, K	Solid		Liquid				
	$V_S, \text{\AA}^3$	$\rho_S, \text{g/cm}^3$	$V_L, \text{\AA}^3$	$\rho_L, \text{g/cm}^3$	$D, 10^{-5} \text{ cm}^2/\text{s}$	$\Delta D/D, \%$	η, cP
3500	132.01	5.03	135.36	4.91	0.04	2.26	-
4000	133.34	4.98	135.71	4.90	0.46	0.23	107.74
4500	134.48	4.94	138.45	4.80	1.77	0.18	31.46
5000	135.79	4.89	139.80	4.75	3.33	0.08	18.51

equation of state by *Stixrude and Karki* [2005]. The discrepancies in pressures between our results and that of *Stixrude and Karki* [2005] are mainly due to the choice of the exchange-correlation functional (i.e., GGA versus LDA) [*Oganov et al.*, 2001a]. This demonstrates the reproducibility of ab initio calculations despite differences between the present computational techniques and those used by *Stixrude and Karki* [2005] (i.e., GGA versus LDA, NPT versus NVT, Car-Parrinello versus Born-Oppenheimer). From linear fits to the data of Figure 1, the estimated thermal expansion coefficients α (in units of 10^{-5} K^{-1}) of solid and molten MgSiO₃ at 120 GPa are 1.88 and 2.15, respectively. The equation of state by *Stixrude and Karki* [2005] gives $\alpha = 1.58$ and 2.11 for solid and molten MgSiO₃ at this pressure.

[13] Our results at 88 GPa with the liquid configuration showed that atoms are diffusive with a diffusion coefficient of $1.14 \times 10^{-5} \text{ cm}^2/\text{s}$. This thermodynamic point (3500 K and 88 GPa) is below the AIMD melting line by *Stixrude and Karki* [2005], but is close to the melting line obtained experimentally by the Berkeley group [*Jeanloz and Kavner*, 1996; *Knittle and Jeanloz*, 1989; *Heinz and Jeanloz*, 1987]. Thus the stability of the liquid in our simulations does not allow us to conclude that 3500 K is above the melting line of the theoretical model employed. However, the finite diffusion coefficient estimated indicates that molten MgSiO₃ is not amorphized. In other words, the liquid is metastable. Liquid metastability in our first-principles simulations is due to supercooling effects [*Allen and Tildesley*, 1987]. The supercooled, molten MgSiO₃ is therefore above the glass transition temperature at 3500 K and 88 GPa. We did not estimate the diffusion coefficients at higher pressures because all the available melting curves suggest that MgSiO₃ can only be solid at these thermodynamic conditions.

[14] Regarding the simulations with liquid configuration: when pressure increases, the atoms approach each other and become nondiffusive. This can be observed by our estimated diffusion coefficients at 88 GPa ($1.14 \times 10^{-5} \text{ cm}^2/\text{s}$) and 120 GPa ($0.04 \times 10^{-5} \text{ cm}^2/\text{s}$). In other words, the undercooled liquid is amorphized. In addition, as pressure increases, the percentage difference of volumes between solid and liquid MgSiO₃ becomes smaller, which indicates a tendency toward density inversion at higher pressures.

[15] In Figure 1 (bottom), the volumes are shown as a function of temperature up to 5000 K. Pressure is fixed at 120 GPa. This is close to the top of the D'' region in the mantle. This pressure is also close to where MgSiO₃ transforms to a postperovskite phase [*Murakami et al.*, 2004]. In this study, our solid state calculations are restricted to the perovskite crystal structure. The volume of the postperov-

skite (CaIrO₃ type) phase is $\sim 1-1.5\%$ less than perovskite [*Oganov and Ono*, 2004; *Tsuchiya et al.*, 2004; *Shieh et al.*, 2006] at deep lower mantle pressures, so this transformation will increase the density contrast between solid and liquid. Because of uncertainties associated with the Clapeyron slope of the transition and the deep mantle geotherm, it is possible that at the base of the mantle, the geotherm will cross back into the perovskite stability field [*Hernlund et al.*, 2005] and thus a comparison of perovskite and liquid densities may still be the relevant case for consideration of the ultralow-velocity zone.

[16] Although melting has not been observed during the simulations, our DFT-GCA calculated results provide an upper bound on the solid volume. The numerical results are given in Table 2. For liquid simulations, the changes of volume and density can be approximately divided into two regions: $T > 4500 \text{ K}$ and $T < 4000 \text{ K}$. The diffusion coefficient decreases from $0.46 \times 10^{-5} \text{ cm}^2/\text{s}$ at 4000 K to $0.04 \times 10^{-5} \text{ cm}^2/\text{s}$ at 3500 K. Thus the molten MgSiO₃ can be regarded as nondiffusive at 3500 K. However, the melt structure at the lower temperatures ($T < 4000 \text{ K}$) and high pressures ($\sim 120 \text{ GPa}$) may not be stabilized within our simulation time ($\sim 10 \text{ ps}$), which results in uncertainties of the estimated diffusion coefficient. In particular, the stability of diffusion in molten MgSiO₃ at 4000 K may be questionable and requires a longer simulation.

3.2. Diffusion Near the Core-Mantle Boundary

[17] In Table 2, we tabulate the estimated diffusion coefficients and viscosities of MgSiO₃ as a function of temperature. Pressure is fixed at 120 GPa. The estimated diffusion coefficient drops drastically as the temperature drops from 4500 K to 4000 K. This is a strong indication of amorphization of molten MgSiO₃. The mean square displacements of molten MgSiO₃ at different temperatures are shown in Figure 2. As seen, the atoms are clearly diffusive at higher temperatures (4500–5000 K). With a pressure shift of 14 GPa (Figure 1), our calculated EOS of molten MgSiO₃ at 3500 K is highly consistent with that of SK05, which was calculated by using LDA. As a result, our simulations of molten MgSiO₃ at 120 GPa correspond to the results of SK05 at 106 GPa. At 106 GPa, the melting temperature determined by SK05 is $\sim 5000 \text{ K}$, with a lower bound of $\sim 4500 \text{ K}$. Hence, despite that melting temperature has not been determined in our work, our simulations provide evidence that MgSiO₃ is diffusive and is above the glass transition temperature at $T > 4500 \text{ K}$.

[18] The mean square displacements of different species of atoms at 5000 K are shown in Figure 3. Results for both solid and liquid are shown. In the solid, Si atoms are bounded by the octahedra formed by the O atoms, and each

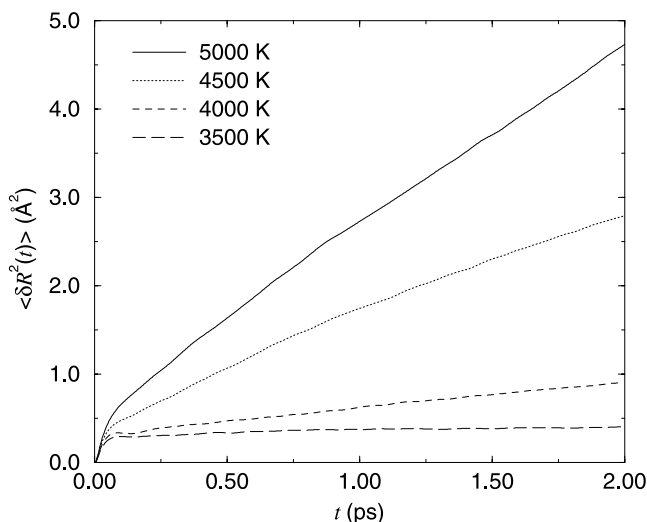


Figure 2. Mean square displacements of molten MgSiO_3 at 120 GPa.

octahedron is then surrounded by 8 Mg atoms. Hence Mg atoms are expected to have a larger vibrational amplitude than that of the other species, and Si atoms are expected to have the smallest vibrational amplitude (Figure 3). In molten MgSiO_3 , the slopes of the mean square displacements of each species are close to that of each other. This suggests the self-diffusion rate of each species is almost the same. However, the diffusion mechanism is beyond the scope of this work and will be the subject of further studies.

4. Discussion and Conclusion

4.1. Density

[19] At 3500 K and 88 GPa, the density of crystalline MgSiO_3 in the perovskite structure is 5% greater than liquid MgSiO_3 whereas the density excess becomes 2.9% at 120 GPa and 5000 K. The transformation to a postperovskite phase would further enhance this density contrast. Thus we find that liquid MgSiO_3 is always less dense than the corresponding solid under conditions encountered within Earth's mantle. This implies that stability of melts in the deep lower mantle requires in addition compositional differences between melt and solid. It is well known on the basis of mineral-melt partitioning data for perovskite that Fe is preferentially partitioned into the melt, and resulting in a higher density of the melt. Hence, in addition to the volume of fusion, Fe enrichment in the melt must be contained when evaluating the stability of melts in an idealized $(\text{Mg}, \text{Fe})\text{SiO}_3$ lower mantle [Knittle, 1998].

[20] The effect of Fe on densities in crystalline and liquid $(\text{Mg}, \text{Fe})\text{SiO}_3$ perovskites can be calculated using known thermoelastic parameters [Jackson, 1998; Kiefer et al., 2002] and assuming that the effect of Fe on density in the liquid is similar to its effect on the solid. For solid $(\text{Mg}, \text{Fe})\text{SiO}_3$ compositions with $\text{Mg}/(\text{Mg} + \text{Fe})$ ratios of 0.90 to 0.95, the solid-liquid Fe partition coefficients required to be in equilibrium with neutrally buoyant melt at 120 GPa and 5000 K range from 0.31 to 0.48. These are within the wide range of reported experimental solid/liquid

partition coefficients ($K = (X_{\text{Mg}}/X_{\text{Fe}})^{\text{liquid}}/(X_{\text{Mg}}/X_{\text{Fe}})^{\text{solid}}$) for perovskite compositions at lower mantle pressures (0.12–0.57) [Ito and Takahashi, 1987; McFarlane et al., 1994; Knittle, 1998]. Thus the combination of the small volume change of fusion determined here with Fe partitioning constraints from experiments suggest that negative or neutrally buoyant melts are plausible in the D'' and ULVZ layers at least with respect to perovskite structured solids. This conclusion is consistent with other recent calculations [Stixrude and Karki, 2005]. Partition coefficients within the experimentally measured range (0.2–0.34) also produce neutrally buoyant melts at 88 GPa and 3500 K. Thus these results suggest that small amounts of neutrally buoyant partial melt in the deep lower mantle could also contribute to the anomalous $\partial \ln V_S / \partial \ln V_P$ observed in this region [Duffy and Ahrens, 1992]. Negative buoyancy under these conditions could instead led to melt pooling in D'' and the ULVZ [Knittle, 1998]. Better constraints on Fe partition coefficients under deep mantle conditions are needed to distinguish between these possibilities.

[21] Extrapolation of the trend in Figure 1 indicates that MgSiO_3 liquid and crystal densities will become equal near 180 GPa. There are few experimental constraints on densities in MgSiO_3 liquids under these extreme conditions. The density change along the Hugoniot in Mg_2SiO_4 upon shock melting at 150 GPa is small and there is a suggestion of enhanced compressibility in the melt [Brown et al., 1987]. More recent shock experiments on MgSiO_3 compositions have suggested that the density of the melt becomes comparable to that of the solid near 120 GPa, and at 170 GPa, the melt density exceeds the solid density [Akins et al., 2004]. However, the shock data near 120 GPa (which are directly comparable to our simulations) have uncertainties that allow melt densities to be as much as several percent less than the solid, and thus they are not necessarily inconsistent with the present results.

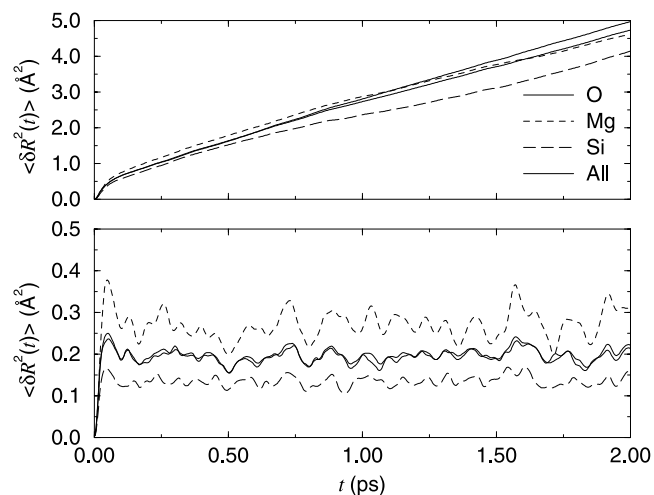


Figure 3. Mean square displacements of (top) molten and (bottom) solid MgSiO_3 at 5000 K and 120 GPa. Solid lines indicate O atoms, dashed lines indicate Mg atoms, long dashed lines indicate Si atoms, and solid bold lines indicate all atoms.

4.2. Diffusivity

[22] The diffusion coefficients we have obtained can be compared to values on similar liquids at lower pressure and temperature conditions. The self-diffusion of Si and O has been measured in a diopside liquid up to 15 GPa and 2573 K [Reid *et al.*, 2001]. The oxygen and silicon diffusivities are similar and reach a value of 9.1×10^{-6} cm²/s at the highest *P-T* conditions. By contrast, our diffusivities are about 2–4 times larger at 120 GPa and 4500–5000 K. In a molecular dynamics study using an empirical potential model, diffusivities were calculated for MgSiO₃ melts at the same temperatures as our study (4500–5000 K) but pressure of 5 GPa [Wasserman *et al.*, 1993]. In this case, the diffusivities of O and Si range from 2 to 4×10^{-5} cm²/s and that for Mg was larger at $7\text{--}10 \times 10^{-5}$ cm²/s. Our bulk values at the same temperature and 120 GPa are $2\text{--}3 \times 10^{-5}$ cm²/s which if the two results are comparable suggests that diffusivities may not be strongly pressure-dependent.

4.3. Viscosity

[23] The viscosities of silicate liquids have been investigated experimentally using a wide variety of techniques at ambient and low pressures [Doremus, 2002; Dingwell, 1998]. However, there are few constraints on the behavior of silica-poor and relatively depolymerized melts that are relevant to melting in the deep Earth [Dingwell *et al.*, 2004]. The viscosity of a diopside (CaMgSi₂O₆) liquid has been determined to high pressures and temperatures using the falling sphere method at 8–13 GPa and 2200–2470 K [Reid *et al.*, 2003]. Recent measurements of the viscosity of peridotite liquids yields values ranging between 19–130 cP at 3–13 GPa and 2043–2523 K [Liebske *et al.*, 2005].

[24] An increase in viscosity with pressure is expected as a result of the reduction in interatomic spacing with compression. However, changes in melt structure resulting in increases in the mean coordination number with increasing pressure lead to decreases in shear viscosity of the melt. When coordination changes are completed, additional pressure increases will once again cause viscosity to increase. The studies of both diopside and peridotite liquids show evidence for decreases in viscosity at high pressures (>8 GPa) suggesting changes in melt structure are important under these conditions [Reid *et al.*, 2003; Liebske *et al.*, 2005]. Recent AIMD simulations [Stixrude and Karki, 2005] indicate that the coordination number increases continuously in MgSiO₃ liquid over a broad compression interval rather than being confined to a limited pressure range. The sensitivity of viscosity to pressure, temperature, and melt structure introduces large uncertainties in any extrapolation of silicate liquid viscosities to deep mantle conditions relevant to the core-mantle boundary region or the base of an early magma ocean. For this reason, computational studies of melt properties are needed for placing constraints on such properties at deep mantle conditions beyond the range of current experiment.

[25] The viscosity of a peridotite liquid was recently measured at 1 bar at both superliquidus and supercooled conditions [Dingwell *et al.*, 2004]. The viscosity near 1850 K was found to be 126 cP. On the basis of the strongly non-Arrhenian temperature dependence observed, it was estimated that extrapolation to 5000 K will yield a viscosity of liquid peridotite of only about 0.3 cP [Dingwell *et al.*,

2004]. This is about 60 times lower than value we obtain for MgSiO₃ liquid at the same temperature but at 120 GPa.

[26] Our simulation results yield broadly similar viscosity values (19–108 cP) at conditions appropriate for D'' (120 GPa, 4000–5000 K) as those observed in the peridotite liquid at low pressures and temperatures. Since the temperature effects on viscosity remain strong at high pressure (Table 2), this would require the viscosity to increase with compression as predicted by Liebske *et al.* [2005] at higher *P* when melt compaction effects begin to dominate over coordination changes.

[27] In summary, we have performed ab initio molecular dynamics simulations to study MgSiO₃, the main mineral composition in the Earth's lower mantle. By applying variable-cell dynamics, we studied both solid perovskite and molten MgSiO₃ in constant *NPT* ensemble without the need for optimizing the cell parameters. At thermodynamic conditions close to that of the core-mantle boundary, we have constrained the viscosity, diffusion coefficient, and density of liquid MgSiO₃.

[28] The next step is to study the diffusion mechanism in molten MgSiO₃ as well as the effect of chemical heterogeneity on the diffusion and melting behavior. With increasing computation power, it is anticipated that the applications of ab initio molecular dynamics can contribute to detailed understanding of mineral physics at the core-mantle boundary.

[29] **Acknowledgments.** J. T. K. Wan acknowledges the financial support from The Croucher Foundation. This work was supported by the NSF. We thank A. Kubo, P. Tangney and A. Trave for valuable discussion. Extensive computation was made at the Keck Computational Materials Science Laboratory at the Princeton Institute for the Science and Technology of Materials (PRISM).

References

- Agee, C. B. (1998), Crystal-liquid density inversions in terrestrial and lunar magmas, *Phys. Earth. Planet. Inter.*, *107*, 63–74.
- Akins, J. A., S.-N. Luo, P. D. Asimow, and T. J. Ahrens (2004), Shock-induced melting of MgSiO₃ perovskite and implications for melts in Earth's lowermost mantle, *Geophys. Res. Lett.*, *31*, L14612, doi:10.1029/2004GL020237.
- Allen, M. P., and D. J. Tildesley (1987), *Computer Simulation of Liquids*, Oxford Univ. Press, New York.
- Bagchi, B. (2001), Relation between orientation correlation time and the self-diffusion coefficient of tagged probes in viscous liquids: A dimensional theory analysis, *J. Comput. Phys.*, *115*, 2207–2211.
- Blöchl, P. E., and M. Parrinello (1992), Adiabaticity in first-principles molecular dynamics, *Phys. Rev. B*, *45*, 9413–9416.
- Brown, J. M., M. D. Furnish, and R. G. McQueen (1987), Thermodynamics for (Mg,Fe)₂SiO₄ from the hugoniot, in *High-Pressure Research in Mineral Physics*, *Geophys. Monogr. Ser.*, vol. 39, edited by M. H. Manghni and Y. Syono, pp. 373–384, AGU, Washington, D. C.
- Car, R., and M. Parrinello (1985), Unified approach for molecular dynamics and density functional theory, *Phys. Rev. Lett.*, *55*, 2471–2474.
- Dingwell, D. B. (1998), Melt viscosity and diffusion under elevated pressures, in *Ultrahigh Pressure Mineralogy*, *Rev. Mineral.*, vol. 37, edited by R. Hemley and D. Mao, pp. 397–424, Mineral. Soc. of Am., Washington, D. C.
- Dingwell, D. B., P. Courtial, D. Giordano, and A. R. L. Nichols (2004), Viscosity of peridotite liquid, *Earth Planet. Sci. Lett.*, *226*, 127–138.
- Doremus, R. H. (2002), Viscosity of silica, *J. Appl. Phys.*, *92*, 7619–7629.
- Duffy, T. S., and T. J. Ahrens (1992), Lateral variation in lower mantle seismic velocities, in *High-Pressure Research in Mineral Physics: Applications to Earth and Planetary Sciences*, edited by Y. Syono and M. H. Manghni, pp. 197–206, Terra Sci., Tokyo.
- Garnero, E. J., S. P. Grand, and D. V. Helmberger (1993), Low *p*-wave velocity at the base of the mantle, *Geophys. Res. Lett.*, *20*, 1843–1846.

- Gezelter, J. D., E. Rabani, and B. J. Berne (1999), Calculating the hopping rate for diffusion in molecular liquids: CS₂, *J. Comput. Phys.*, *110*, 3444–3452.
- Heinz, D. L., and R. Jeanloz (1987), Measurement of the melting curve of Mg_{0.9}Fe_{0.1}SiO₃ at lower mantle conditions and its geophysical implications, *J. Geophys. Res.*, *92*, 11,437–11,444.
- Helmberger, D. V., S. D. Ni, L. X. Wen, and J. Ritsema (2000), Seismic evidence for ultralow-velocity zones beneath Africa and eastern Atlantic, *J. Geophys. Res.*, *105*, 23,865–23,878.
- Hemlund, J. W., C. Thomas, and P. J. Tackley (2005), A doubling of the post-perovskite phase boundary and structure of the Earth's lower mantle, *Nature*, *434*, 882–886.
- Hohenberg, P., and W. Kohn (1964), Inhomogeneous electron gas, *Phys. Rev.*, *136*, B864–B871.
- Hoover, W. G. (1985), Canonical dynamics: Equilibrium phase-space distributions, *Phys. Rev. A*, *31*, 1695–1697.
- Ito, E., and E. Takahashi (1987), Melting of peridotite at uppermost lower mantle conditions, *Nature*, *328*, 514–517.
- Jackson, I. (1998), Elasticity, composition, and temperature of the Earth's lower mantle: A reappraisal, *Geophys. J. Int.*, *134*, 291–311.
- Jeanloz, R., and A. Kavner (1996), Melting criteria and imaging spectro-radiometry in laser-heated diamond-cell experiments, *Philos. Trans. R. Soc. London, Ser. A*, *354*, 1279–1305.
- Karki, B. B., L. Stixrude, S. J. Clark, M. C. Warren, G. J. Ackland, and J. Crain (1997), Elastic properties of orthorhombic MgSiO₃ perovskite at lower mantle pressures, *Am. Mineral.*, *82*, 635–638.
- Karki, B. B., R. M. Wentzcovitch, S. de Gironcoli, and S. Baroni (2000), Ab initio lattice dynamics of MgSiO₃ perovskite at high pressure, *Phys. Rev. B*, *62*, 14,750–14,756.
- Karki, B. B., D. Bhattarai, and L. Stixrude (2006), First-principles calculations of the structural, dynamical and electronic properties of liquid MgO, *Phys. Rev. B*, *73*, 174–208.
- Kiefer, B., L. Stixrude, and R. M. Wentzcovitch (2002), Elasticity of (Mg, Fe)SiO₃-Perovskite at high pressures, *Geophys. Res. Lett.*, *29*(11), 1539, doi:10.1029/2002GL014683.
- Knittle, E. (1998), The solid/liquid partitioning of major and radiogenic elements at lower-mantle pressures: Implications for the core-mantle boundary region, in *The Core-Mantle Boundary Region, Geodyn. Ser.*, vol. 28, edited by W. Gurnis et al., pp. 119–130, AGU, Washington D. C.
- Knittle, E., and R. Jeanloz (1989), Melting curve of (Mg,Fe)SiO₃ perovskite to 96 GPa: Evidence for a structural transition in lower mantle melts, *Geophys. Res. Lett.*, *16*, 421–424.
- Kohn, W., and L. J. Sham (1965), Self-consistent equations including exchange and correlation effects, *Phys. Rev. A*, *140*, 1133–1138.
- Liebske, C., B. Schmickler, H. Terasaki, B. T. Poe, A. Suzuki, K. Funakoshi, R. Ando, and D. C. Rubie (2005), Viscosity of peridotite liquid up to 13 GPa: Implications for magma ocean viscosities, *Earth Planet. Sci. Lett.*, *240*, 589–604.
- Louie, S. G., S. Froyen, and M. L. Cohen (1982), Nonlinear ionic pseudopotentials in spin-density functional calculations, *Phys. Rev. B*, *26*, 1738–1742.
- March, N. H., and M. P. Tosi (1999), Generalized Stokes-Einstein relation for liquid metals near freezing, *Phys. Rev. E*, *60*, 2402–2403.
- Matsukage, K. N., Z. C. Jing, and S. Karato (2005), Density of hydrous silicate melt at the conditions of Earth's deep upper mantle, *Nature*, *438*, 488–491.
- McFarlane, E. A., M. J. Drake, and D. C. Rubie (1994), Element partitioning between Mg-perovskite, *Geochim. Cosmochim. Acta*, *58*, 5161–5172.
- Murakami, M., K. Hirose, K. Kawamura, N. Sata, and Y. Ohishi (2004), Post-perovskite phase transition in MgSiO₃, *Science*, *304*, 855–858.
- Nosé, S. (1984), A molecular-dynamics method for simulations in the canonical ensemble, *Mol. Phys.*, *52*, 255–268.
- Oganov, A. R., and S. Ono (2004), Theoretical and experimental evidence for a post-perovskite phase of MgSiO₃ in Earth's D'' layer, *Nature*, *430*, 445–448.
- Oganov, A. R., J. P. Brodholt, and G. D. Price (2001a), Ab initio elasticity and thermal equation of state of MgSiO₃ perovskite, *Earth Planet. Sci. Lett.*, *184*, 555–560.
- Oganov, A. R., J. P. Brodholt, and G. D. Price (2001b), The elastic constants of MgSiO₃ perovskite at pressures and temperatures of the Earth's mantle, *Nature*, *411*, 934–937.
- Ohtani, E. (1985), The primordial terrestrial magma ocean and its implication for stratification of the mantle, *Earth Planet. Sci. Lett.*, *38*, 70–80.
- Ohtani, E., and M. Maeda (2001), Density of basaltic melt at high pressure and stability of melt at the base of the lower mantle, *Earth Planet. Sci. Lett.*, *193*, 69–75.
- Parrinello, M., and A. Rahman (1980), Crystal structure and pair potentials: A molecular-dynamics study, *Phys. Rev. Lett.*, *45*, 1196–1199.
- Perdew, J. P., K. Burke, and M. Ernzerhof (1996), Generalized gradient approximation made simple, *Phys. Rev. Lett.*, *77*, 3865–3868.
- Reid, J. E., B. T. Poe, D. C. Rubie, N. Zotov, and M. Wiedenbeck (2001), The self-diffusion of silicon and oxygen in diopside (CaMgSi₂O₆) liquid up to 15 GPa, *Chem. Geol.*, *174*, 77–86.
- Reid, J. E., A. Suzuki, K. I. Funakoshi, H. Terasaki, B. T. Poe, D. C. Rubie, and E. Ohtani (2003), The viscosity of CaMgSi₂O₆ liquid at pressures up to 13 GPa, *Phys. Earth Planet. Inter.*, *139*, 45–54.
- Revenaugh, J., and R. Meyer (1997), Seismic evidence of partial melt within a possibly ubiquitous low-velocity layer at the base of the mantle, *Science*, *277*, 670–673.
- Rigden, S. M., T. J. Ahrens, and E. M. Stolper (1984), Densities of liquid silicates at high pressures, *Science*, *226*, 1071–1074.
- Sakamaki, T., A. Suzuki, and E. Ohtani (2006), Stability of hydrous melt at the base of the Earth's upper mantle, *Nature*, *439*, 192–194.
- Shieh, S. R., T. S. Duffy, A. Kubo, G. Shen, V. B. Prakapenka, N. Sata, K. Hirose, and Y. Ohishi (2006), Equation of state of the post-perovskite phase synthesized from a natural (Mg,Fe)SiO₃ orthopyroxene, *Proc. Natl. Acad. Sci. U. S. A.*, *103*, 3039–3043.
- Solomatov, V. S. (2000), Fluid dynamics of a terrestrial magma ocean, in *Origin of the Earth and Moon*, edited by R. M. Canup and K. Righter, pp. 323–338, Univ. of Ariz. Press, Tucson.
- Stevenson, D. J. (1989), Formation and early evolution of the Earth, in *Mantle Convection: Plate Tectonics and Global Dynamics*, edited by W. R. Peltier, pp. 817–873, Gordon and Breach, New York.
- Stixrude, L., and B. Karki (2005), Structure and freezing of MgSiO₃ liquid in Earth's lower mantle, *Science*, *310*, 297–299.
- Suzuki, A., and E. Ohtani (2003), Densities of liquid silicates at high pressures, *Phys. Chem. Miner.*, *30*, 449–456.
- Troullier, N., and J. L. Martins (1991), Efficient pseudopotentials for plane-wave calculations, *Phys. Rev. B*, *43*, 1993–2006.
- Tsuchiya, T., J. Tsuchiya, K. Umemoto, and R. A. Wentzcovitch (2004), Phase transition in MgSiO₃ perovskite in the Earth's lower mantle, *Earth Planet. Sci. Lett.*, *224*, 241–248.
- Vanderbilt, D. (1990), Soft self-consistent pseudopotentials in a generalized eigenvalue formalism, *Phys. Rev. B*, *41*, 7892–7895.
- Wasserman, E. A., D. A. Yuen, and J. R. Rustad (1993), Molecular dynamics study of the transport properties of perovskite melts under high temperature and pressure conditions, *Earth Planet. Sci. Lett.*, *114*, 373–384.
- Wen, L. X., and D. V. Helmberger (1998), Ultra-low velocity zones near the core-mantle boundary from broadband PKP precursors, *Science*, *279*, 1701–1703.
- Wen, L. X., P. Silver, D. James, and R. Kuehnel (2001), Seismic evidence for a thermo-chemical boundary at the base of the Earth's mantle, *Earth Planet. Sci. Lett.*, *189*, 141–153.
- Wentzcovitch, R. M., B. B. Karki, M. Cococcioni, and S. de Gironcoli (2004), Thermoelasticity of MgSiO₃ perovskite: Insights on the nature of the Earth's lower mantle, *Phys. Rev. Lett.*, *92*, 018501.
- Williams, Q., and E. J. Garnero (1996), Seismic evidence for partial melt at the base of Earth's mantle, *Science*, *273*, 1528–1530.
- Zwanzig, R. (1983), On the relation between self-diffusion and viscosity of liquids, *J. Comput. Phys.*, *79*, 4507–4508.

R. Car, Department of Chemistry, Princeton University, Princeton, NJ 08544, USA.

T. S. Duffy, Department of Geosciences, Princeton University, Princeton, NJ 08544, USA. (duffy@princeton.edu)

S. Scandolo, Abdus Salam International Centre for Theoretical Physics, Strada Costiera 11, 34100 Trieste, Italy.

J. T. K. Wan, Department of Physics, Chinese University of Hong Kong, Shatin, New Territories, Hong Kong. (jwan@phy.cuhk.edu.hk)